Simultaneous Evaporation of Cu and Sn from Liquid Steel

SUNG-HOON JUNG and YOUN-BAE KANG

In order to understand evaporation refining of tramp elements in molten ferrous scrap, Cu and Sn, a series of experiments were carried out using liquid–gas reaction in a levitation melting equipment. Effect of S and C, which are abundant in hot metal from ironmaking process, was examined and analyzed by employing a comprehensive evaporation kinetic model developed by the present authors (Jung *et al*. in Metall Mater Trans B 46B:250–258, 2014; Jung *et al*. in Metall Mater Trans B 46B:259–266, 2014; Jung *et al*. in Metall Mater Trans B 46B:267–277, 2014; Jung and Kang in Metall Mater Trans B 10.1007/s11663-016-0601-5, 2016). Evaporation of Cu and Sn were treated by evaporation of individual species such as Cu(g), CuS(g), Sn(g), and SnS(g), along with CS_2(g). Decrease of Cu and Sn content in liquid steel was in good agreement with the model prediction. Optimum conditions of steel composition for the rapid evaporation of Cu and Sn were proposed by utilizing the model predictions.

DOI: 10.1007/s11663-016-0699-5

I. INTRODUCTION

IN order to develop an efficient and economic process for recycling of ferrous scrap, it is indispensable to understand thermodynamic and kinetic aspects of tramp elements in the ferrous scrap dissolving in liquid iron/steel. Those can be used to interpret various proposed refining processes such as evaporation, chlorination, and sulfide flux refining, in particular for Cu and Sn refining.[5–7] Kinetic information of the evaporation is considered to be practically important because it is valuable in estimating process time for the evaporation refining of Cu and Sn from liquid iron/steel dissolving the ferrous scrap.

The present authors have reported the evaporation mechanism of Sn and Cu, and effect of S and C, present in liquid iron/steel, on the evaporation was elucidated by analyzing experimental data obtained by the present authors, when mass transfers in gas and in liquid phases were not rate determining steps.[1–4] It was shown that S has two roles for the evaporation of Cu or Sn: (1) accelerating the evaporation by forming CuS(g) or SnS(g), and (2) decelerating the evaporation by blocking reaction sites as being a typical surface active element. It was also shown that C has two roles: (1) accelerating the evaporation by increasing activity coefficient of Cu and S simultaneously, or Sn and S simultaneously, and (2) decelerating the evaporation by forming CS_2(g), by which chances for Cu to form CuS(g) or Sn to form SnS(g) are lowered. Based on these mechanisms found in Fe-Cu-C-S alloy system and Fe-Sn-C-S alloy system, respectively, evaporation kinetic models for each system were developed.[1–4] Model prediction in each system was shown to be in good agreement with measured experimental data.

In the present article, the developed kinetic models for evaporation of each tramp element (Cu or Sn) are extended into a general case where evaporations of Cu and Sn are considered simultaneously in liquid iron containing C and S (Fe-Cu-Sn-C-S). If the model developed for each system (Fe-Cu-C-S[4] and Fe-Sn-C-S[1–3]) can be simply extended and this is consistent with experimental data (concentration variations of Cu and Sn in liquid Fe-Cu-Sn-C-S alloys), then it may be concluded that (1) the extended kinetic model for the evaporation of Cu and Sn can be used to predict evaporation kinetics with confidence, (2) evaporation of Cu and Sn are coupled on the basis of the evaporation mechanism proposed in the previous studies by the present authors, and (3) the evaporation mechanism in sub-system is validated even at higher order system.

II. EXPERIMENTAL

A series of liquid–gas reactions was carried out in order to measure the evaporation rate of Cu and Sn under a condition where mass transfers in gas phase and liquid phase were not a rate-controlling step. Experimental details are almost similar to those employed in the previous studies of the present authors.[1–4]

A. *Sample Preparation*

Several alloys made of Fe-Cu-Sn, Fe-Cu-Sn-S, and Fe-C-Cu-Sn-S were prepared in an induction melting

SUNG-HOON JUNG, formerly with the Graduate Institute of Ferrous Technology, Pohang University of Science and Technology, Pohang, Kyungbuk 37673, Republic of Korea, is now Senior Researcher with the Gwangyang Process Research Group, Technical Research Laboratories, POSCO, Gwangyang, Cheonnam 57807, Republic of Korea. YOUN-BAE KANG, Associate Professor, is with the Graduate Institute of Ferrous Technology, Pohang University of Science and Technology. Contact e-mail: ybkang@postech.ac.kr
Manuscript submitted February 10, 2016.
Article published online May 31, 2016.

furnace under purified Ar atmosphere. Electrolytic iron with FeS powder (99.9 mass pct, Strem Chemicals, USA), Cu powder (99 mass pct, Aldrich, USA), and granule of Sn (99.99 mass pct, RND 172 Korea Company, Korea) was melted in alumina or graphite crucibles at 1873K (1600 °C). Small portions of the melt were sampled by quartz tubes to obtain bars of 4×10^{-3} m diameter. Samples for the evaporation experiment using an electromagnetic levitation technique were prepared by cutting and grinding those bars into small pieces (approximately to the weight of $6 \pm 0.1 \times 10^{-4}$ kg).

B. *Experimental Procedure and Chemical Analysis*

Experimental equipment and procedure used in the present study are the same as those given in the previous articles.[1–4] An electromagnetic levitation technique was used by an RF generator (30 kW, 260 kHz) in order to make the reaction between gas and liquid alloy. During the levitation and melting, mainly an Ar-4 pctH_2 gas mixture was flown into the reaction chamber made of a quartz tube (ID: 18 mm) in order to prevent accidental oxidation during the experiment. The flow rate of deoxidized gas mixture was kept at 1 L minute^{-1}. Temperature of the levitated droplet was controlled manually and was measured by a two-color pyrometer. In the present study, all experiments were carried out at 1873 ± 283 K (1600 ± 10 °C). After a predetermined time was passed, the droplet was quenched into a water in a copper mold.

Cu and Sn concentrations of the samples were analyzed by Inductively Coupled Plasma spectrometer (ICP-AES, Thermo Scientific ICAP 6500), and C and S concentrations were analyzed by C/S combustion analysis method (LECO CS844). The mass of the sample collected from each levitation run was not sufficient for the chemical analyses of Cu, Sn, S, and C, respectively. Therefore, the experiment with the same condition was repeated in order to collect enough material for chemical analysis.

All experimental conditions employed in the present study are listed in Table I. It was confirmed that liquid/gas phase mass transport were not the rate-controlling step.[1,4]

III. RESULTS AND DISCUSSION

A. *Evaporation Reactions and Rate Equations*

Let us consider a liquid alloy composed of Fe-Cu-Sn-C-S. The following evaporations are considered [1–4]:

$$\underline{\mathrm{Cu}} = \mathrm{Cu(g)}, \qquad [1]$$

$$\underline{\mathrm{Cu}} + \underline{\mathrm{S}} = \mathrm{CuS(g)}, \qquad [2]$$

$$\underline{\mathrm{Sn}} = \mathrm{Sn(g)}, \qquad [3]$$

$$\underline{\mathrm{Sn}} + \underline{\mathrm{S}} = \mathrm{SnS(g)}, \qquad [4]$$

$$\underline{\mathrm{C}} + 2\underline{\mathrm{S}} = \mathrm{CS_2(g)}. \qquad [5]$$

Rate of concentration variations of Cu, Sn, and S due to the evaporation are formulated as

$$\frac{\mathrm{d[pct\ Cu]}}{\mathrm{d}t} = -\frac{A}{V}\left(k_{\mathrm{Cu}}\frac{f_{\mathrm{Cu}}}{f^{\circ}_{\mathrm{Cu}}}[\mathrm{pct\ Cu}] + k_{\mathrm{CuS}}\frac{f_{\mathrm{Cu}}}{f^{\circ}_{\mathrm{Cu}}}[\mathrm{pct\ Cu}]\frac{f_{\mathrm{S}}}{f^{\circ}_{\mathrm{S}}}[\mathrm{pct\ S}]\right), \qquad [6]$$

$$\frac{\mathrm{d[pct\ Sn]}}{\mathrm{d}t} = -\frac{A}{V}\left(k_{\mathrm{Sn}}\frac{f_{\mathrm{Sn}}}{f^{\circ}_{\mathrm{Sn}}}[\mathrm{pct\ Sn}] + k_{\mathrm{SnS}}\frac{f_{\mathrm{Sn}}}{f^{\circ}_{\mathrm{Sn}}}[\mathrm{pct\ Sn}]\frac{f_{\mathrm{S}}}{f^{\circ}_{\mathrm{S}}}[\mathrm{pct\ S}]\right), \qquad [7]$$

$$\frac{\mathrm{d[pct\ S]}}{\mathrm{d}t} = -\frac{A}{V}\left(\begin{array}{l}\dfrac{\mathrm{M_s}}{\mathrm{M_{Cu}}}k_{\mathrm{CuS}}\dfrac{f_{\mathrm{Cu}}}{f^{\circ}_{\mathrm{Cu}}}[\mathrm{pct\ Cu}]\dfrac{f_{\mathrm{S}}}{f^{\circ}_{\mathrm{S}}}[\mathrm{pct\ S}] \\ +\dfrac{\mathrm{M_s}}{\mathrm{M_{Sn}}}k_{\mathrm{SnS}}\dfrac{f_{\mathrm{Sn}}}{f^{\circ}_{\mathrm{Sn}}}[\mathrm{pct\ Sn}]\dfrac{f_{\mathrm{S}}}{f^{\circ}_{\mathrm{S}}}[\mathrm{pct\ S}] \\ +k_{\mathrm{CS2}}[\mathrm{pct\ C}][\mathrm{pct\ S}]^2\end{array}\right), \qquad [8]$$

Table I. Experimental Conditions Employed in the Present Study

Exp. No.[a]	Gas Species	Flow Rate (L min^{-1})	[Pct Cu]$_0$	[Pct Sn]$_0$	[Pct S]$_0$	[Pct C]$_0$
CuSn1	Ar-4 pctH_2	1.00	0.465	0.187	0.0006[b]	0
CuSnS1	Ar-4 pctH_2	1.00	0.469	0.186	0.058	0
CuSnS2	Ar-4 pctH_2	1.00	0.467	0.174	0.132	0
CuSnS3	Ar-4 pctH_2	1.00	0.423	0.176	0.204	0
CuSnS4	Ar-4 pctH_2	1.00	0.532	0.164	0.297	0
CuSnS5	Ar-4 pctH_2	1.00	0.488	0.137	0.456	0
CCuSnS1	Ar-4 pctH_2	1.00	0.444	0.178	0.320	4.85

All experiments were carried out at 1873 K (1600 °C). Dimension of droplet: radius (m) = 2.74×10^{-3}, surface area (m^2) = 9.4×10^{-5}, volume (m^3) = 8.57×10^{-8}, density (kg m^{-3}) = 7000.

[a]CuSn: Fe-Cu-Sn alloy, CuSnS: Fe-Cu-Sn-S alloy, CCuSnS: Fe-C-Cu-Sn-S alloy.

[b]No S was introduced in the sample.

where [pct i], f_i, f_i°, and M_i are mass percent of element i, activity coefficient of the i, activity coefficient of i at zero C content, and molecular weight of the i (kg mol^{-1}), respectively. t, A, and V are reaction time (seconds), area of reaction surface (m^2), and volume of melt (m^3), respectively. Overall evaporation rate of Cu is contributed by individual evaporations of Cu(g) and CuS(g). Similarly, overall evaporation rate of Sn is contributed by individual evaporations of Sn(g) and SnS(g). And overall evaporation of S, which affects the evaporation rate of CuS(g) and SnS(g), is contributed by individual evaporations of CuS(g), SnS(g), and CS_2(g), respectively. As discussed previously,[3, 4] variation of C content, Δ[pct C], due to the evaporation of CS_2, is not explicitly considered. This is because Δ[pct C] = 0.5 × M_C/M_S Δ[pct S] ≈ 0.19 × Δ[pct S], which is relatively small compared to C content in hot metal (*i.e.*, [pct C]$_0$ ≈ 5). On the other hand, the effects of the C content on activity coefficients of Cu, Sn, and S are taken into account by the ratio of activity coefficient (f_i/f_i°). When [pct C] = 0, the ratio becomes unity, and the evaporation of CS_2(g) is naturally ignored. When C content is as high as it saturation, *i.e.*, [pct C] ≈ 5, the ratio of Cu, Sn, and S are set to f_{Cu}/f_{Cu}° = 2.1, f_{Sn}/f_{Sn}° = 3.7, f_S/f_S° = 3.5, respectively.[3,4] Ratios of molecular weight, M_S/M_{Cu} and M_S/M_{Sn}, appear in Eq. [8], because k_{CuS} and k_{SnS} were obtained for [pct Cu] and [pct Sn], respectively.[1,2,4] For the calculation of [pct S], the constants need to be corrected by the ratio of molecular weight. On the other hand, similar correction is not necessary for k_{CS2} which was obtained for [pct S] directly.[3]

k_j's in Eqs. [6] to [8] are the apparent rate constants for the evaporation of the species j (j = Cu(g), CuS(g), Sn(g), SnS(g), and CS_2(g), respectively), and those are further expressed as [1–4]

$$k_{Cu} = \left(\frac{k_{Cu}^R}{1 + K_S (f_S/f_S^\circ)[\text{pct S}]} + k_{Cu}^r \right), \quad [9]$$

$$k_{CuS} = \frac{\rho}{100 M_S} \left(\frac{k_{CuS}^R}{1 + K_S (f_S/f_S^\circ)[\text{pct S}]} + k_{CuS}^r \right), \quad [10]$$

$$k_{Sn} = \left(\frac{k_{Sn}^R}{1 + K_S (f_S/f_S^\circ)[\text{pct S}]} + k_{Sn}^r \right), \quad [11]$$

$$k_{SnS} = \frac{\rho}{100 M_S} \left(\frac{k_{SnS}^R}{1 + K_S (f_S/f_S^\circ)[\text{pct S}]} + k_{SnS}^r \right), \quad [12]$$

$$k_{CS2} = \frac{\rho^2}{10000 M_C M_S} \left(\frac{k_{CS2}^R}{1 + K_S (f_S/f_S^\circ)[\text{pct S}]} + k_{CS2}^r \right), \quad [13]$$

where K_S is an adsorption coefficient of S onto surface of liquid Fe (40 at 1873 K (1600 °C)[8]). k_j^R and k_j^r are chemical reaction rate constant and residual rate constant of the evaporation of the species j (j = Cu(g), CuS(g), Sn(g), SnS(g), and CS_2(g), respectively).[1–4] ρ is the density of the melt, and 7000 kg m^{-3} was used in the present study. Derivation steps for these equations can be found in Reference 4. All the k_j^R and k_j^r at 1873 K (1600 °C) were already obtained in previous investigations for each sub-system, and they are listed in Table II.

Decrease of [pct Cu] and [pct Sn], along with [pct S], can be calculated using Eqs. [6] to [8] with the help of Eqs. [9] to [13]. In order to solve Eqs. [6] to [8], a simple numerical approach was used with a time step, Δt = 5 seconds. At each time t, rate constants are first calculated using Eqs. [9] to [13]. These are then substituted into Eqs. [6] to [8] in order to get instantaneous evaporation rates of Cu, Sn, and S, respectively. Finite variation of concentrations of Cu, Sn, and S are then calculated during the time step Δt, in order to get the concentrations of them after the time step. These steps are repeated for desired time.[2–4] This calculation for liquid steel containing Cu and Sn simultaneously is indeed a prediction using the rate constants evaluated for each sub-system.[1–4]

B. *Experimental Results and Comparison with the Model Predictions*

Figure 1 shows concentrations of Cu, Sn, and S in several Fe-Cu-Sn-S alloys of various initial S contents ([pct S]$_0$) (0.0006 to 0.456) at 1873 K (1600 °C), quenched after the melting/evaporation at each time (up to 1800 seconds). Concentrations of all three elements decreased continuously regardless of [pct S]$_0$. It is most evident that [pct Sn] decreased faster when [pct S]$_0$ was higher. On the other hand, although [pct Cu] decreased, the increase of [pct S]$_0$ did not enhance evaporation rate of Cu. For example, [pct Cu] after 1800 seconds when [pct S]$_0$ was 0.0006 (Figure 1(a)) was lesser than 0.1, but that of [pct S]$_0$ = 0.132 (Figure 1(c)) was greater than 0.1. In order to confirm this observation, concentrations of Cu, Sn, and S at 1800 seconds were normalized by their initial concentrations and plotted at each [pct S]$_0$. This is shown in Figure 2. It is clearly seen that the increase of [pct S]$_0$ increased the evaporation rate of Sn monotonously ([pct Sn]$_{t\ =\ 1800\ \text{seconds}}$ is low at high [pct S]$_0$), but it is not true for the case of Cu. Increasing the [pct S]$_0$ up to 0.2 resulted in slower evaporation (higher [pct Cu]$_{t\ =\ 1800\ \text{seconds}}$). Further increase of the [pct S]$_0$ could enhance the evaporation rate of Cu. This is consistent with the report by the present authors for Cu evaporation in Fe-Cu-S/Fe-Cu-C-S alloys.[4] This was attributed to the fact that S has two opposite roles in the evaporation of Cu as mentioned earlier in this communication proposed by the present authors.[4] The same roles are expected in the case of the evaporation of Sn. However, the evaporation of Sn was gradually enhanced by the increase of [pct S]$_0$. This can be attributed to the

Table II. Rate Constants for Evaporation of Each Gas Species at 1873 K (1600 °C) Evaluated in the Previous Investigations[1–4]

j	k_j^R	k_j^r	Refs.
Cu	8.00×10^{-7} m s^{-1}	4.00×10^{-7} m s^{-1}	[4]
CuS	1.37×10^{-9} m^4 mol^{-1} s^{-1}	4.11×10^{-10} m^4 mol^{-1} s^{-1}	[4]
Sn	3.49×10^{-7} m s^{-1}	0 m s^{-1}	[2]
SnS	1.00×10^{-8} m^4 mol^{-1} s^{-1}	1.40×10^{-9} m^4 mol^{-1} s^{-1}	[1]
CS_2	4.24×10^{-12} m^7 mol^{-2} s^{-1}	4.24×10^{-16} m^7 mol^{-2} s^{-1}	[3]

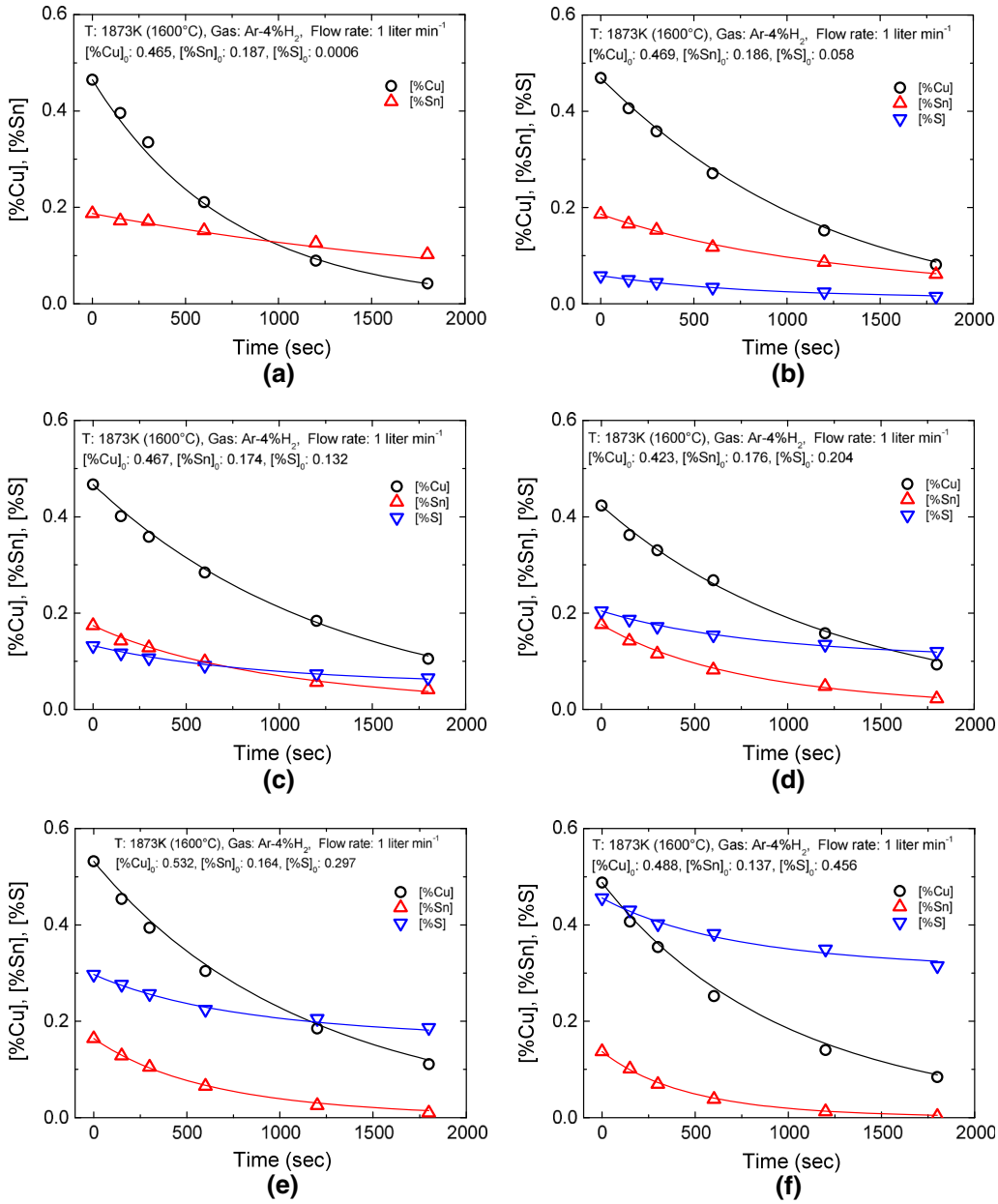

Fig. 1—Decrease of [pct Cu], [pct Sn], and [pct S] in several Fe-Cu-Sn-S alloys of different initial concentrations at 1873 K (1600 °C). Lines are calculated using evaporation model for Fe-Cu-Sn-S alloy developed in the present study, Eqs. [6] to [8].

fact that SnS(g) is more stable than CuS(g), as the Gibbs energy of formation of SnS(g) is much negative than that of CuS(g) (See Table III). Figure 3 shows the number of moles of evaporated Sn (Δn_{Sn}) and that of S (Δn_S), respectively. From the experimental data shown by various symbols, it is seen that $\Delta n_S > \Delta n_{Sn}$ for all cases. Therefore, there should have been CuS(g) evaporation in addition to SnS(g) evaporation. Also it is seen

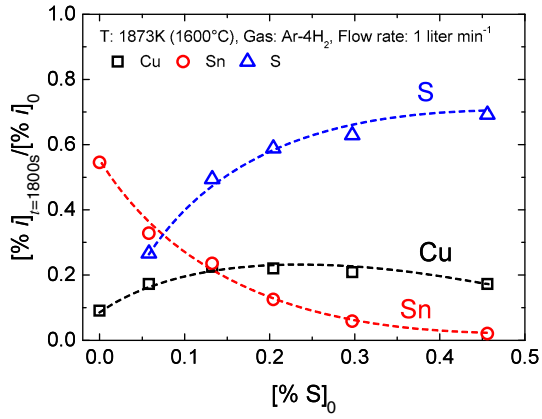

Fig. 2—Normalized concentration of Cu, Sn, and S in the alloys at 1800 s shown in Fig. 1.

Table III. Gibbs Energy for Formation of CuS(g) and SnS(g) at 1873 K (1600 °C)[10]

Reaction	Gibbs Energy of Reaction (J mol^{-1})
Cu(l) + 1/2S$_2$(g) = CuS(g)	+79,100
Sn(l) + 1/2S$_2$(g) = SnS(g)	−58,226

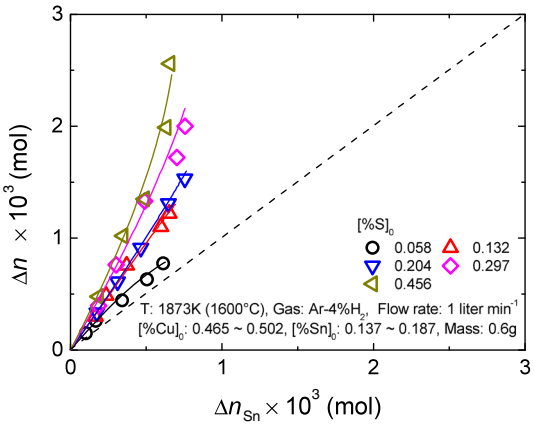

Fig. 3—Number of moles of Sn and S removed from the alloys (mass of the alloys: 6×10^{-4} kg) shown in Fig. 1. Lines are calculated using evaporation model for Fe-Cu-Sn-S alloy developed in the present study, Eqs. [6] to [8].

that Δn_S kept increasing, while Δn_{Sn} ceased to increase. This implies that earlier stage of the evaporation was governed by the SnS(g), while later stage of the evaporation (when [pct Sn] had been decreased) was governed by the CuS(g).

The above experimental finding was compared with the model calculations using Eqs. [6] to [12] at [pct C] = 0, with the rate constants shown in Table I. The calculated results are in the forms of [pct Cu], [pct Sn], and [pct S] in Figure 1, and of Δn_{Sn} and Δn_S in Figure 3. It is seen that very good agreement with the experimental data was obtained.

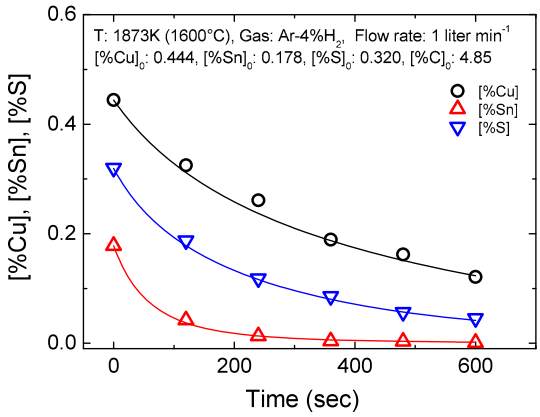

Fig. 4—Decrease of [pct Cu], [pct Sn], and [pct S] in an Fe-Cu-Sn-C-S alloy at 1873 K (1600 °C). Lines are calculated using evaporation model for Fe-Cu-Sn-C-S alloy developed in the present study, Eqs. [6] to [8].

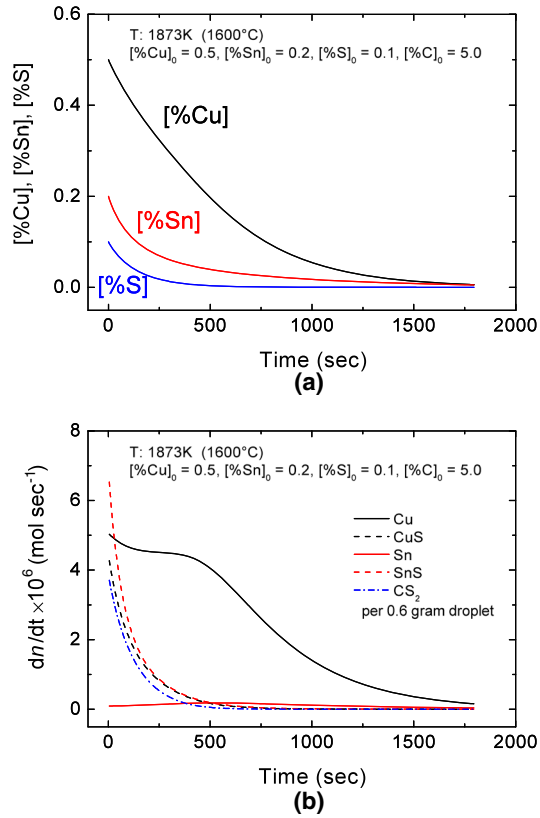

Fig. 5—Model prediction for concentrations of individual elements, and evaporation rate of individual species for Fe-0.5-0.2Sn-5C-0.1S at 1873 K (1600 °C).

Further experiment was carried for the evaporation when C presents in the liquid alloy. Initial C content ([pct C]$_0$) was 4.85, almost close to C saturation.[9] The obtained experimental data are shown in Figure 4. It is seen that Sn content decreased more rapidly at the early stage of the evaporation, compared to that shown in Figure 1(e) where [pct S]$_0$ in two samples were similar.

The effect of C on the evaporation of Sn was already discussed in Reference 3. C increased f_{Sn} and f_S simultaneously, and consequently, driving force for the Reaction [4] was increased. Although a driving force of the Reaction [2] could also be increased, the evaporation of Cu was not accelerated as much as Sn, because CuS(g) is less favorable compared to SnS(g) as mentioned before. Solid curves shown in Figure 4 are the calculated results using Eqs. [6] to [13], taking into account CS_2(g) evaporation. Simultaneous consideration of (1) evaporation of five species (Cu(g), Sn(g), CuS(g), SnS(g), and CS_2(g)); (2) surface adsorption of S; and (3) increasing activity coefficients of Cu, Sn, and S by C was fully considered for this calculation. Very good agreement with the experimental data lends strong support for the evaporation mechanism proposed by the present authors through a series of researches, and the evaporation kinetic model developed by the present authors.[1–4]

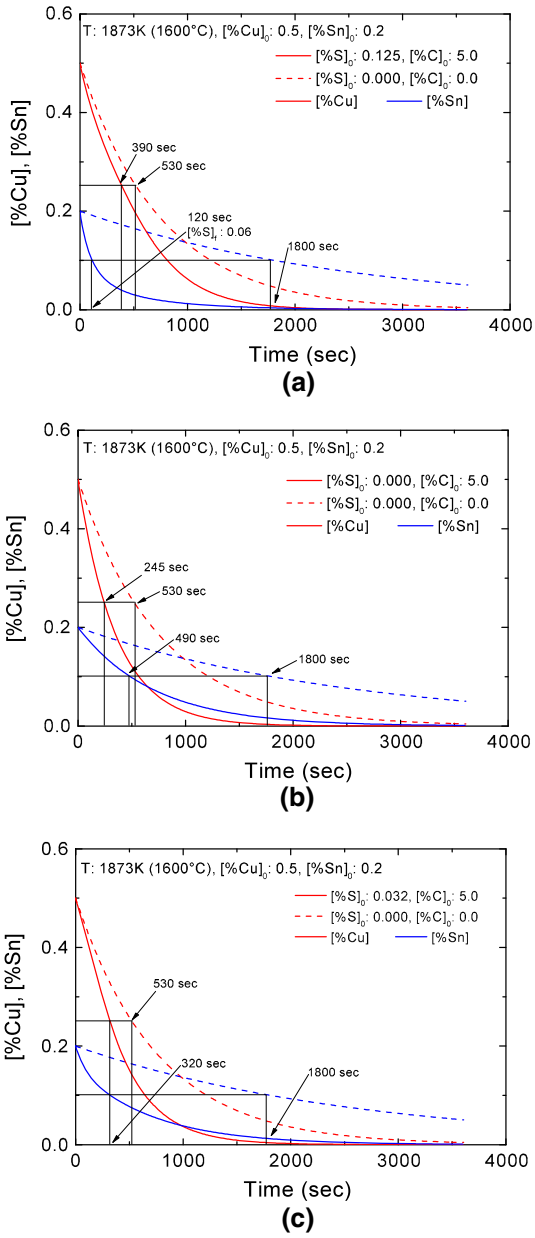

Fig. 6—Decrease of [pct Cu] and [pct Sn] in liquid steels of various initial compositions at 1873 K (1600 °C) predicted by the evaporation model developed in the present study.

Actual evaporating species could be predicted by the evaporation kinetic model. Figure 5 shows an example calculation for an alloy of Fe-0.5Cu-0.2Sn-5.0C-0.1S at 1873 K (1600 °C). Concentrations of Cu, Sn, and S are shown in Figure 5(a). Figure 5(b) shows evaporation rates of individual species. First and second terms in the right-hand side of Eq. [6] were considered as the evaporation rates of Cu(g) and CuS(g), respectively. Similarly, those of Eq. [7] were considered as the evaporation rates of Sn(g) and SnS(g), respectively. Last term of Eq. [8] was considered as the evaporation rate of CS_2(g). This prediction shows that SnS(g) is the fastest evaporating species initially, even though [pct Sn]$_0$ was lesser than [pct Cu]$_0$. Evaporation rate of Sn(g) is very low. On the other hand, evaporation rate of Cu(g) is always greater than that of CuS(g), due to low stability of the CuS(g). The rates of sulfides (CuS(g), SnS(g), and CS_2(g)) decreased rapidly as [pct S] decreased.

C. *Application of the Kinetic Model for the Evaporation*

Finally, the developed evaporation kinetic model was utilized for a practical application. One of the most important factors for a refining process of Cu and Sn by the evaporation is accelerating the evaporation rates of Cu and Sn as fast as possible. As discussed in previous studies,[2] S plays an important role in the acceleration of the evaporation rate of Sn. Having high S content in liquid steel is beneficial to increase the evaporation rate of Sn, and may be for Cu at considerably high S content. On the other hand, final S content after the refining process should be as low as a level that can be readily desulfurized by a conventional desulfurization process. Therefore, it is necessary to find an optimal initial S content for faster Cu and Sn refining. A number of calculations were conducted in order to seek the optimal condition for Cu and Sn removal by Eqs. [6], [7], and [8] under the conditions employed in the present study [1873 K (1600 °C) and fast mass transfer in the liquid and in the gas]. It is assumed that [pct Cu]$_0$ and [pct Sn]$_0$

Table IV. Time Required for Refining of 50 Pct Cu and Sn in Liquid Alloys ([Pct Cu]$_0$: 0.5, [Pct Sn]$_0$: 0.2) at 1873 K (1600 °C)

	Composition	deCu Time (s)	deSn Time (s)
Liquid Fe	[pct C]$_0$: 0.0, [pct S]$_0$: 0.0	530	1800
Maximum Cu evaporation	[pct C]$_0$: 5.0, [pct S]$_0$: 0.0	245 (2.2)	490 (3.7)
Optimal Cu and Sn evaporation	[pct C]$_0$: 5.0, [pct S]$_0$: 0.032	320 (1.7)	320 (5.7)
Maximum Sn evaporation	[pct C]$_0$: 5.0, [pct S]$_0$: 0.125	390 (1.4)	120 (15)

were set to be 0.5 and 0.2, respectively. Furthermore, the final S content after the refining ($[pct\ S]_f$) is to be less than 0.06, after 50 pct of Cu and Sn are evaporated. The 0.06 as $[pct\ S]_f$ is a typical S level in hot metal after ironmaking process, before hot metal pretreatment.

The calculation results are shown in Figure 6, which show optimized conditions after a series of calculations. In order to accelerate the Sn evaporation rate regardless of the Cu evaporation rate, it is required to increase $[pct\ C]_0$ from 0 to 5, and $[pct\ S]_0$ from 0 to 0.125, respectively, as shown in Figure 6(a). This increased the Sn evaporation rate 15 times (1800 to 120 seconds for 50 pct evaporation). However, this increased the Cu evaporation time only 1.4 times. This is partly due to too high S content, and this seems not so beneficial for Cu evaporation. In order to accelerate the Cu evaporation rate regardless of the Sn evaporation rate, it is required to increase $[pct\ C]_0$ from 0 to 5, while $[pct\ S]_0$ is set to 0, respectively, as shown in Figure 6(b). This increased the Cu evaporation rate 2.2 times (530 to 245 seconds for 50 pct evaporation). However, this increased the Sn evaporation time only 3.7 times. Some conditions between these two may be thought. As seen in Figure 6(c), when $[pct\ C]_0$ and $[pct\ S]_0$ are 5 and 0.032, respectively, the evaporation rates of Cu and Sn increased 1.7 and 5.4 times, respectively. The calculation result is summarized in Table IV. From the model calculation, it is shown that initial compositions of C and S are key factors for control refining time for Cu and Sn by evaporation.

IV. CONCLUSION

In summary, the present article describes the evaporation kinetics of Cu and Sn in liquid Fe alloys containing C and S. It was confirmed by a number of gas–liquid experiments that previously reported evaporation mechanism for Cu[4] and Sn,[1–3] respectively, could be applied to the simultaneous evaporation of Cu and Sn. Previously developed evaporation kinetic models for Cu[4] and Sn[1–3] could be extended into a system containing Cu and Sn, simultaneously. Prediction by the kinetic model has been shown to be reliable by comparison with the experimental data obtained in the present study. Example applications were shown to give a guide for refining time for scrap recycling process.

ACKNOWLEDGMENT

This research was financially supported by POSCO Ltd. through Steel Innovation Program.

REFERENCES

1. S.-H. Jung, Y.-B. Kang, J.-D. Seo, J.-K. Park, and J. Choi: *Metall. Mater. Trans. B*, 2014, vol. 46B, pp. 250–58.
2. S.-H. Jung, Y.-B. Kang, J.-D. Seo, J.-K. Park, and J. Choi: *Metall. Mater. Trans. B*, 2014, vol. 46B, pp. 259–66.
3. S.-H. Jung, Y.-B. Kang, J.-D. Seo, J.-K. Park, and J. Choi: *Metall. Mater. Trans. B*, 2014, vol. 46B, pp. 267–77.
4. S.-H. Jung and Y.-B. Kang: *Metall. Mater. Trans. B.*, 2016, DOI:10.1007/s11663-016-0601-5.
5. L. Savov and D. Janke: *ISIJ Int.*, 2000, vol. 40 (2), pp. 95–104.
6. C. Wang, T. Nagasaka, M. Hino, and S. Ban-Ya: *ISIJ Int.*, 1991, vol. 31 (11), pp. 1300–08.
7. H.G. Katayama, T. Momono, M. Doe, and H. Saitoh: *ISIJ Int.*, 1994, vol. 34 (2), pp. 171–76.
8. K. Sekino, T. Nagasaka, and R.J. Fruehan: *ISIJ Int.*, 2000, vol. 40, pp. 315–21.
9. K. Shubhank and Y.-B. Kang: *CALPAHD*, 2014, vol. 45, pp. 127–37.
10. FT53 compound database, FactSage (http://www.factsage.com).